behavior was observed for the mode located at point S. However, a slight decrease in the secondary amplitude (transition $R \rightarrow Q$) leads to the instability gain $g_{II} \approx 2\sqrt{|a|(1-\lambda)(|a_{cr1}| - |a|)/|a_{cr1}|(1+\lambda)}$, $\lambda < 1$, $|a| < |a_{cr1}|$, and the SLM gets unstable [Fig. 2(b)]. Another type of unstable evolution is shown in Fig. 2(c). It takes place for SLM located in region III with the gain $g_{III} \approx \sqrt{(a - a_{cr2})/2}$.

The asymmetric SLM propagates stable if the ratio of peak amplitudes A/B exceeds some critical value. Therefore, a slight change in the peak amplitude in the vicinity of this point destroys the mode. Because of an "intrinsic bias" of the mode, this SLM decays more rapidly than the symmetric twisted modes. Hence, using such modes in all-optical signal processing seems to be also promising, because less power is needed to switch the output state.

1. A. Aceves *et al.*, Phys. Rev. E **53**, 1172 (1996) (and references therein).

QMB4 — 9:15 am

Directional coupling with optical vortex soliton pair

C.T. Law, X. Zhang, G.A. Swartzlander, Jr.,* *Department of Electrical Engineering and Computer Science, University of Wisconsin, Milwaukee, Wisconsin 53201*

An optical vortex is a distinctive waveform that has a dark circular core on a bright background. Seen from head on, a beam with an optical vortex appears as a bright doughnut of light. The dark core is the result of destructive interference caused by a 2π phase ramp above the core, another characteristic of optical vortex. Very similar to hurricanes or tornadoes, optical vortices in linear medium[1] eventually dissipate. In other words, diffraction causes expansion of vortex core and washes away vortices. Owing to the special intensity profile of vortices, linear optical vortices have been used in trapping and guiding small particles.[2] In a nonlinear medium, such as self-defocusing Kerr material, the nonlinear refractive index induced by the vortex intensity profile counteracts diffraction. As a result, a stable and stationary core with well-defined size is formed inside a light beam. Because the core is immune from instability and its size remains constant with propagation distance, this optical vortex is the only known cylindrical soliton in Kerr media,[3] so-called optical vortex solitons (OVSs).

We have demonstrated the propagation of an OVS in the center of a green Ar ion laser beam in a self-defocusing nonlinear medium. The dark core of an OVS has actually a grade refractive-index profile, which is the imprint of the OVS in the nonlinear medium. Inside the dark core where there is no light, the refractive index maintains its linear value, n_0, while the refractive index under the influence of the bright background is reduced to a smaller value, $n_0 - |n_2|I_\infty$, where I_∞ is the background intensity, and n_2 is the nonlinear refractive-index coefficient. In our first experiment, the guiding of an He-Ne (red) beam within an OVS was demonstrated. The guiding of a light beam of different polarization with an OVS is also possible.[4]

The light-induced fiber provides a means for light-light interaction, such as optical switching and modulation.[5] Moreover, the well-defined core size of an OVS enables a natural extension of hydrodynamics to optics. The fluidlike motion of OVS has been demonstrated experimentally,[6] with phase and intensity profile of an OVS behaving like the flow potential and density of a fluid, respectively. One way to induce OVS motion is to introduce another OVS. Owing to the interaction between two vortices, they will either spiral round each other (if they have the same circulation directions) or drift together (if they have opposite circulation directions). Another method is to modify the background intensity and leads to attraction or repulsion between vortices.

We have performed numerical experiments that simulate the copropagation of OVS pairs with a weak guided beam of various intensity profiles. Our results confirm that OVS pairs with the same circulation direction rotate about the center of axis between the two vortices. Their rate of rotation with respect to propagation distance is close to the theoretical limit, $2/k_0 d^2$, where k_0 is the wave number, and d is the separation between two vortices. This limit becomes exact if the core size is infinitesimally small. In other words, the rotation strength decreases as the core size increases.

Our numerical experiments also demonstrate that the weak guided beam follows the rotation of the OVS. If the propagation distance is long enough, we can realize a spatial switch with more than 90°. Moreover, each vortex in an OVS pair behaves like an isolated entity in terms of waveguiding when the spacing between vortices is more than five times the core size. When the spacing between vortices is small, complete switch over of guided beam from one OVS to another, i.e., directional coupling, is possible. The directional coupling can enhance the spatial switching effect under certain conditions. Various means, including wavelength of the guided beam, spacing, and guided beam size, to optimize the directional coupling as well as the spatial switching effect will be discussed.

This work was supported by the National Science Foundation.

*Department of Physics, Worcester Polytechnic Institute, Worcester, Massachusetts 01609-2280

1. N.B. Baranova, A.V. Mamaev, N.F. Pilipetsky, V.V. Shkunov, B. Ya. Zel'dovich, J. Opt. Soc. Am. **73**, 525 (1983).
2. K.T. Gahagan, G.A. Swartzlander, Jr., Opt. Lett. **21**, 827–829 (1996).
3. G.A. Swartzlander, Jr., C.T. Law, Phys. Rev. Lett. **69**, 2503 (1992); R.Y. Chiao, I.H. Deutsch, J.C. Garrison, E.M. Wright, in *Serge Akhmanov: A Memorial Volume*, H. Walther, ed. (Adam Hilger, Bristol, 1992); A.W. Snyder, I. Poladian, D.J. Mitchell, Opt. Lett. **17**, 789 (1992).
4. C.T. Law, G.A. Swartzlander, Jr., CHAOS **4**, 1759 (1994).
5. G.A. Swartzlander, Jr., D.L. Drugan, N. Hallak, M.O. Freeman, C.T. Law, Laser Phys. **5**, 704 (1995).
6. G.A. Swartzlander, Jr., D. Rozas, Z.S. Sacks, *Fluid-Like Motion of Optical Vortices*, Phys. Rev. Lett. (to be published).

QMC — 8:00 am–10:00 am
Room 270–276

Cavity QED/Trapped Atoms

G. Rempe, *Universitat Konstanz, Germany, Presider*

QMC1 (Invited) — 8:00 am

Real-time cavity QED with single atoms

C.J. Hood, T.W. Lynn, H. Mabuchi, M.S. Chapman, J. Ye, H.J. Kimble, *Caltech 12-33, Pasadena, California 91125*

The use of laser-cooling techniques in optical cavity QED[1] effects a dramatic separation of dynamical timescales, with the coherent interaction rate g_0 dominating over both the cavity field decay rate κ and the atomic dipole decay rate $\gamma_\perp$, which are in turn much larger than rates T^{-1} associated with atomic motion through the spatially varying cavity eigenmode. Below we describe two separate ongoing experiments that explore phenomena uniquely accessible in this regime of true coupling.

Photon-covalent binding of one atom and an optical cavity: A very small high-finesse optical cavity gives us the highest coupling g_0 in an optical system to date: $(g_0, \kappa, \gamma_\perp, T^{-1})/2\pi =$ (120, 40, 2.6, 0.002) MHz. Our first experiment exploits this strong coupling to confine single atoms in a cavity field with $\lesssim$1 photon. Sub-photon intracavity fields can be used to trap atoms because weak excitation by a coherent probe tuned to $\Delta \approx -g_0$ gives rise to a pseudo-potential with depth $\hbar g_0/k_B \approx 7$ mK $\gtrsim$

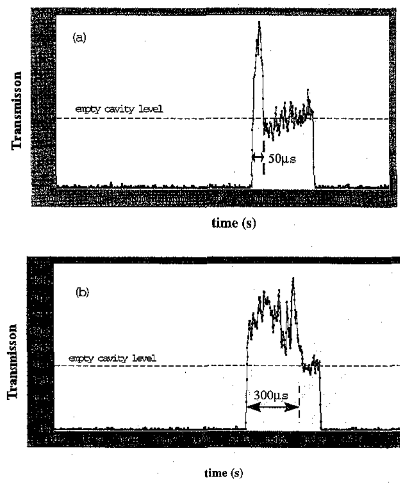

QMC1 **Fig. 1.** Example of atom trapping using the quantized cavity field. The probe beam shown has $\Delta/2\pi = -100$ MHz and is triggered ON by the entrance of an atom into the cavity mode, as discussed in the text. (a) An atom transit where mechanical effects are not important (kinetic energy dominates coupling strength). (b) A localized atom: the atom stays strongly coupled for $\approx$300 μs, after which it exits the cavity and the probe transmission returns to the lower empty cavity level. Maximum dwell times in the absence of mechanical effects are $T \approx 100$ μs.

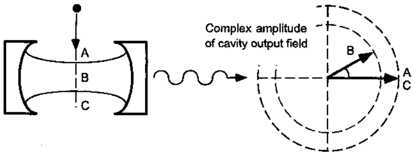

QMC1 Fig. 2. Real-time evolution of the complex field amplitude, brought by single atom transits. A,B,C represent atom positions. Larger detunings from the atomic resonance will elicit more dominant responses in the phase quadrature.

$KE_{atom}{}^2$. In this context, the quantity $\hbar g_0/k_B$ may be interpreted as a covalent atom-cavity binding energy associated with the oscillatory exchange of a single photon. Experimentally, an atom entering the cavity mode causes a drop in transmission of a first probe beam close to resonance; this signal is used to trigger OFF the resonant beam and trigger ON a second probe beam at $\Delta \approx g_0$ to create a trapping potential. Figure 1 shows an example of an atom which has been held in the cavity field for >300 μs, whereas the longest possible transit times expected without mechanical effects are $\simeq 100$ μs. Such data demonstrate the use of strong coupling to exercise significant control over the system's evolution.

Our continuing work addresses the issue of lengthening the atom-cavity interaction time in order to perform arbitrary coherent manipulation of the system. Atom dwell times in the cavity may be increased by cooling the atomic motion in the cavity mode structure. One possible mechanism involves a Sisyphus-like force induced by the cavity's finite response time to a moving atom.[5] Another avenue for cooling is to use our real-time atomic trajectory information to feed back to the atom-cavity system by modulating the well depth to cool the atom. Yet another approach to long interaction times would be to trap the atom via a dipole trapping scheme with far-detuned probe light. In general our investigations of this system are enabled by the realization of a very high single-atom cooperativity $C_1 \equiv g_0^2\,(2\kappa\gamma_\perp)^{-1} \approx 70$. Detection of light leaving the system via cavity decay yields dynamical information which can be used to achieve real-time control of the coupled atom-cavity system.

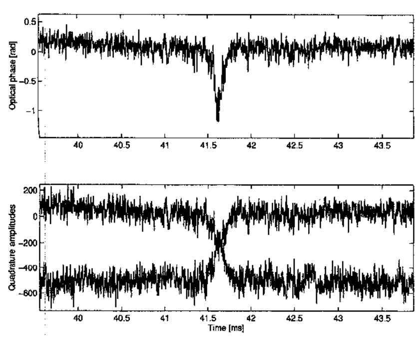

QMC1 Fig. 3. Simultaneous recording of both quadratures of the complex amplitude of the cavity output field (10 kHz filter bandwidth). An optical phase shift of 1 rad is the result of a single atom transit with the probe detuned by −10 MHz.

Continuous measurement of single-atom trajectories: In an independent apparatus with $(g_0, \kappa)/2\pi = (11, 3.5)$ MHz, the cavity leakage field is continuously observed to estimate the intracavity motion of individual atoms. In hopes of eventually reaching the Standard Quantum Limit for monitoring the position of a free mass, we minimize the measurement back action on the CM motion by detuning the probe field from atomic resonance.[3] The experimental protocol then involves determination of the phase of the output field with shot-noise-limited accuracy and bandwidth. Our technical achievements in this regard should enable investigation of the strong conditioning of system evolution on measurement results and the realization of *quantum* feedback control.[4]

Here we report the first measurement of the real-time evolution of the complex field amplitude brought by single atom trasits (see Fig. 2). Figure 3 shows the variation in time of both quadrature amplitudes (simultaneously recorded) of the light transmitted through the cavity, as well the resultant optical phase for a single atom transit event. In this particular measurement, the cavity and laser were both detuned −10 MHz from the Cs resonance. Notice the 1 radian optical phase shift caused by a single atom. At −50 MHz detuning we observe a phase shift of 0.5 rad and a signal-to-noise ratio about 3 at 300 kHz bandwidth, very near the shot noise limit. With improved control over the initial atomic center-of-mass states, the achieved SNR-bandwidth should enable direct observation of single-atom CM oscillations within potential wells associated with the dipole force exerted by the cavity field itself (≈5−10 photons).

1. H. Mabuchi *et al.*, Opt. Lett. **21**, 1393 (1996).
2. A.S. Parkins, unpublished notes (1995).
3. P. Storey *et al.*, Phys. Rev. Lett. **68**, 472 (1992).
4. H.M. Wiseman *et al.*, Phys. Rev. Lett. **70**, 548 (1993).
5. P. Horak *et al.*, Phys. Rev. Lett. **79**, 4974 (1997).

QMC2 8:30 am

Engineering the vibronic coupling of a trapped atom

R.L. de Matos Filho, W. Vogel, *Arbeitsgruppe Quantenoptik, Fachbereich Physik, Universität Rostock, Universitätsplatz 3, D - 18051 Rostock, Germany*

The recent progress in trapping and cooling of atoms allowed us to prepare and to measure various nonclassical states of atomic motion.[1] These methods make use of the laser-assisted vibronic interaction of the trapped atom. The interaction Hamiltonian for the laser being resonant to the kth vibrational sideband reads in the interaction picture as[2]

$$\hat H_{\rm int} = \hbar\Omega_L \hat A_{21} \hat f_k(\hat n)\hat a^k + H.c., \qquad (1)$$

where $\hat f_k(\hat n)$ depends on the vibrational number operator $\hat n = \hat a^\dagger \hat a$ as

$$\hat f_k(\hat n) = e^{-\eta^2/2}\sum_{l=0}^{\infty}\frac{(i\eta)^{2l+k}}{l!(l+k)!}\frac{\hat n!}{(\hat n - l)!}. \qquad (2)$$

Here, $\hat A_{ij}\,(i, j = 1, 2)$ and $\hat a$, respectively, are the electronic (two-level) flip operator and the annihilation operator of a quantum of the vibrational motion, η is the Lamb-Dicke parameter, and Ω_L is the Rabi frequency. The dependence of the Hamiltonian on the vibrational number operator opens several applications, including quantum nondemoliton measurements, quantum computing, and nonlinear coherent states. However, these applications are limited by the given form of the function $\hat f_k(\hat n)$.

To overcome this limitation, we present a scheme that allows one to engineer the excitation dependence of the Hamiltonian.[1] It consists in the excitation of the kth vibrational sideband of the atom by N lasers of the same frequency but of arbitrary Rabi frequencies Ω_j and Lamb-Dicke parameters $\eta_j (j = 1, \ldots, N)$. The latter can be controlled by the geometry of excitation. In this case the Hamiltonian reads

$$\hat H_{\rm int} = \hbar\Omega_R \hat A_{21} \hat F_k(\hat n)\hat a^k + H.c., \qquad (3)$$

Ω_R is a reference Rabi frequency and

$$\hat F_k(\hat n) = \sum_{l=0}^{\infty}\left[\sum_{j=0}^{N} e^{-\eta_j^2/2}\frac{\Omega_j}{\Omega_R}\frac{(i\eta_j)^{2l+k}}{l!(l+k)!}\right] \times \frac{\hat n!}{(\hat n - l)!}. \qquad (4)$$

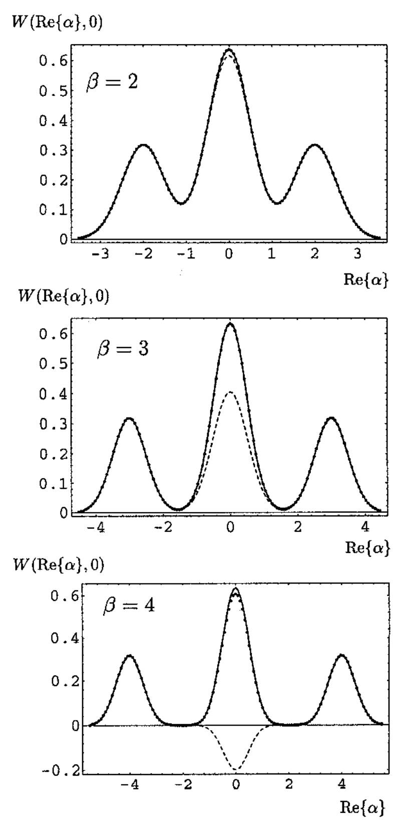

QMC2 Fig. 1. The Wigner function $W(\mathrm{Re}\{\alpha\}, \mathrm{Im}\{\alpha\})$ at $\mathrm{Im}\{\alpha\} = 0$ is shown for an even coherent state for different values of the amplitude β: theoretical curve (full line), measurement using the engineering method (dotted line), and measurement using the method of Ref. 3 (shaded line).